

RSC Advances



This is an *Accepted Manuscript*, which has been through the Royal Society of Chemistry peer review process and has been accepted for publication.

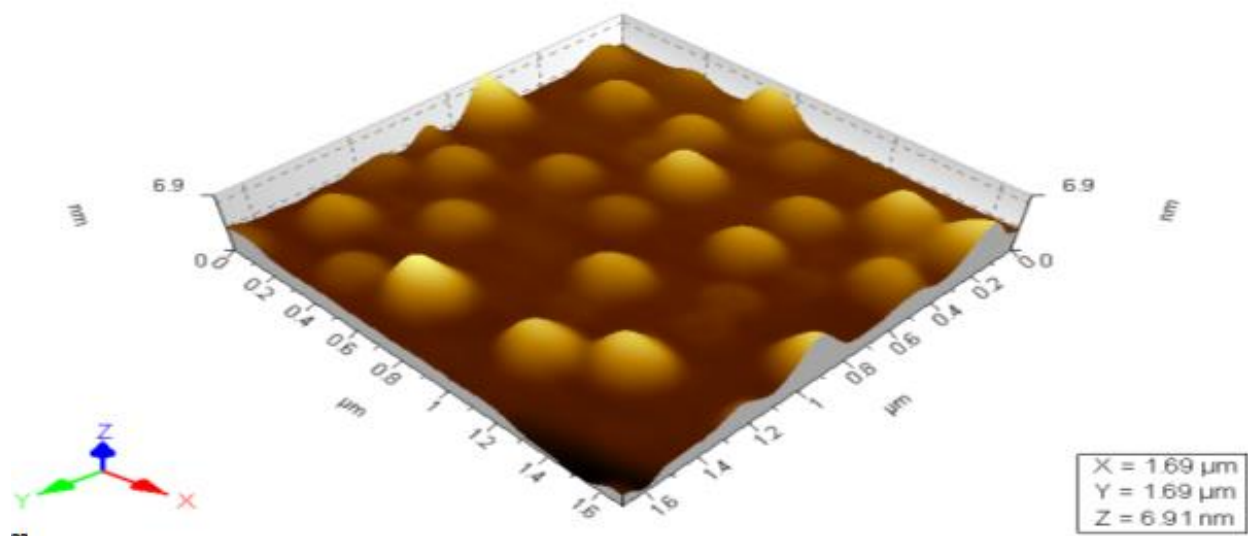
Accepted Manuscripts are published online shortly after acceptance, before technical editing, formatting and proof reading. Using this free service, authors can make their results available to the community, in citable form, before we publish the edited article. This *Accepted Manuscript* will be replaced by the edited, formatted and paginated article as soon as this is available.

You can find more information about *Accepted Manuscripts* in the [Information for Authors](#).

Please note that technical editing may introduce minor changes to the text and/or graphics, which may alter content. The journal's standard [Terms & Conditions](#) and the [Ethical guidelines](#) still apply. In no event shall the Royal Society of Chemistry be held responsible for any errors or omissions in this *Accepted Manuscript* or any consequences arising from the use of any information it contains.

Paliperidone loaded spherical solid lipid nanoparticles

Sacheen Kumar and Jaspreet K. Randhawa*[†]



Gelucire® 50/13, a macrogol glyceride was used as a surfactant for the preparation and stabilization of paliperidone loaded Capmul® GMS-50K matrix based solid lipid nanoparticles (SLNs). Homogeneously distributed paliperidone did not affect the crystal structure of the lipid matrix in SLNs.

Paliperidone loaded spherical solid lipid nanoparticles

Cite this: DOI:

Sacheen Kumar and Jaspreet K. Randhawa*[†]

Received 00th January 2012,
Accepted 00th January 2012

DOI:

Gelucire® 50/13, a macrogol glyceride was used as a surfactant for the preparation and stabilization of paliperidone loaded Capmul® GMS-50K matrix based solid lipid nanoparticles (SLNs). Z-average particle size of SLNs was found to be directly proportional to the concentration of Gelucire® 50/13. 10 mg/ml was found to be optimum amount of Gelucire® 50/13 for the formation of a monolayer around SLNs. SLNs with the optimised amount of surfactant was characterised thoroughly by transmission electron microscopy (TEM) and atomic force microscopy (AFM). X-ray diffraction (XRD) and FTIR spectroscopy analysis showed that the lipid matrix crystallised in the triclinic form in SLNs. Homogeneously distributed paliperidone did not affect the crystal structure of the lipid matrix in SLNs. Entrapment efficiency of the optimised formulation was 75% with 7% drug loading.

Introduction

Last decade witnessed a proficient interest towards drug targeting of the brain. Antipsychotic drugs have a market share of \$22-25 Bn annually [1-3]. Central nervous system (CNS) disorders are increasing among the population worldwide [3]. The neurological disorders are multi-systemic and are difficult to treat as portal entry to brain is restricted on account of its anatomical and physiological barriers [4]. The growing knowledge about the brain capillary endothelium and the discovery of specific mechanisms for the uptake of substances enables the development of various strategies to enhance the drug delivery rate into the brain [5]. Among the different strategies, nanodrugs are promising candidates for drug delivery to the brain due to their potential in encapsulating drugs. Among the many nanodrug carrier systems, SLNs have many advantages over the others. SLNs have been used for bio-availability enhancement of drugs, controlled release and drug targeting [6]. Due to the high biocompatibility of lipids, all the existing administration routes are virtually possible for SLNs.

Among the CNS disorders, Schizophrenia is a brain disorder that is usually treated with antipsychotic drugs which include “typical” or “first generation” and “atypical” or “second generation” drugs. Paliperidone or 9-hydroxyrisperidone is the most recently available atypical antipsychotic drug. It is the primary active metabolite of risperidone, a well-established second-generation antipsychotic drug [7-9]. Paliperidone has been developed as an extended-release(ER) tablet formulation and is approved in the US and EU for the acute and maintenance treatments of schizophrenia in adults.

Formulating the surfactant coating of nanoparticles was considered as a potential approach to improve brain drug

uptake of paliperidone. In our previous work we have used Capmul® GMS-50K as a lipid and sodium deoxycholate as a surfactant to encapsulate paliperidone [9]. Capmul® GMS-50K is the trade name of glycerolmono stearate and is a mono-triglyceride of hydrogenated vegetable oil. Sodium deoxycholate is well reported to enhance permeability across blood brain barrier(BBB) [10]. We could achieve the entrapment efficiency of 55% with 4.15% of drug loading in lipid matrix.

In the present study Gelucire®50/13 has been used as the non-ionic surfactant while keeping the lipid carrier same for making SLNs loaded with paliperidone. Gelucire® 50/13 is a glyceride of polyethylene glycol (PEG) and fatty acids. Gelucire® 50/13 is well known to enhance the oral bioavailability of drugs [11-14]. Gelucires could facilitate the production of SLNs with narrow size distribution with enhanced drug encapsulation for poorly soluble drugs [15]. Gelucire® 50/13 stabilized SLNs remains stable at different pH values. But sodium deoxycholate stabilized SLNs may get destabilized at acidic pH [16]. Gelucire® 50/13 is generally recognised as safe (GRAS) by the FDA, whereas sodium deoxycholate do not fall in the category. Non-ionic surfactants such as Gelucire® 50/13 are much less toxic than the anionic surfactants [15]. Drug loaded SLNs were prepared by ultrasound assisted melt homogenization and structural characterization was done by using XRD and FTIR spectroscopy. Morphology of the SLNs was characterized by dynamic light scattering (DLS), TEM and AFM imaging.

Results and Discussion

Capmul® GMS-50K and Gelucire® 50/13 based SLNs were stabilized by self-emulsification process through ultrasound assisted melt homogenization. Optimization of process parameters like temperature, stirring speed, stirring

time, ultra sonication power, ultra-sonication time and cooling conditions were done previously and were maintained constant for the synthesis of SLNs [17]. Effect of the surfactant on the particle size and shape was studied carefully and the results are discussed in the following sections.

Effect of surfactant content, presence of drug and temperature on SLNs

Without using surfactants, it was impossible to prepare SLNs with Capmul® GMS-50K. The effect of varying the quantity of Gelucire® 50/13 on the particle size was studied by DLS which gave Z-average size of SLNs. Z-average size and PDI recorded with respect to Gelucire® 50/13 content present and are reported in Table 1. The particle size of SLNs decreased from 392 nm to 100 nm with increase in concentration of Gelucire® 50/13 from 2.5 mg/ml to 20 mg/ml. There was no specific trend in PDI. It was observed that the particle size of SLNs decreased sharply with increasing Gelucire® 50/13 content upto 10 mg/ml, which is equivalent to 1:1 weight ratio of the surfactant and the lipid. This is because the particle size of dispersions depends strongly on the nominal surfactant concentration that is needed to form a dense adsorption monolayer on the particles. A plot of z-average size against Gelucire® 50/13 content gave a hyperbolic fit (Figure S1, electronic supplementary information). The hyperbolic fit showed that particle size decreased sharply with increasing concentration of Gelucire® 50/13 until 10 mg/ml (1:1 wt./wt.). The particle size of SLNs decreased relatively less abruptly with the change in Gelucire® 50/13 content at concentrations above 10 mg/ml. This may be because the surfactant concentration needed for the formation of a dense monolayer is approximately 10 mg/ml. A similar trend was prophesied in the model proposed by Tcholakova et. al.[18]. High concentrations of surfactants above the concentration required for monolayer formation controls the particle size by preventing the drop-drop coalescence [19]. Zeta potential was not affected by Gelucire® 50/13 content, as it was found to be around -19 to -21 mV for all the samples as shown in Table 1. It may be due to the non-ionic nature of the surfactant used. Above 20 mg/ml of Gelucire® 50/13 content gelling of sample starts to a large extent and hence higher concentrations were not used. Thus the minimum surfactant concentration that is needed for obtaining a monolayer covered SLN was determined as 10 mg/ml. Further studies on paliperidone loaded Gelucire® 50/13 stabilized SLNs were performed with this optimum concentration.

Table 1 Effect of Gelucire 50/13 concentration on the Z-average size and Polydispersity index (PDI) which were measured by PCS/DLS of SLNs

Sr. No.	Ratio (wt./wt.) of Gelucire® 50/13 & Capmul® GMS-50K	Z-average Size (nm)	PDI	Zeta Potential (mV)
1.	1:4	392.5	0.44	-19.4
2.	2:4	223.3	0.66	-20.1
3.	3:4	187.5	0.58	-20.0
4.	1:1	163.2	0.67	-21.1
5.	5:4	147.8	0.63	-20.3
6.	3:2	133.8	0.46	-21.1

7.	7:4	119.2	0.46	-19.8
8.	2:1	100.3	0.68	-20.2

When we used Sodium Deoxycholate in our previous work, SLNs with particle size of 200 nm was obtained with a weight ratio of 1:4 of the surfactant and the lipid. Whereas with Gelucire® 50/13 as surfactant, particle size of SLNs was around 392 nm at the same weight ratio. However, particle size of SLNs could be lowered further even upto 100 nm with Gelucire® 50/13 by using higher concentration of the surfactant. However, higher concentration of sodium deoxycholate could not be used in SLNs due to the relative high toxicity of it.

The effect of presence of drug on particle size on the optimized formulation was also studied using DLS. From the data reported in Figure S2a and S2b (electronic supplementary information) it is clear that there is apparent increase in z-average particle size when drug is present in SLNs. However, this observation is not sufficient to conclude that presence of drug increases the particle size. The apparent increase in z-average particle size was due to slight increase in the population of micron sized particles that was present even in the absence of drug.

The effect of temperature on the size of SLNs was studied by DLS to understand the thermal stability of the SLNs. The temperature of the suspension of SLNs in water was increased gradually from 20 °C to 65 °C by varying the temperature of the sample chamber of DLS instrument. The particle size was measured after equilibrating the sample for 120 s at the pre-set temperature. A plot of particle size versus temperature is shown in Figure 1. Temperature did not appear to have any effect on the particle size of SLNs till 56 °C. The particle size starts to decrease when the temperature is raised beyond 56 °C. This may be due change in phase of SLNs in the dispersion at 56 °C [20].

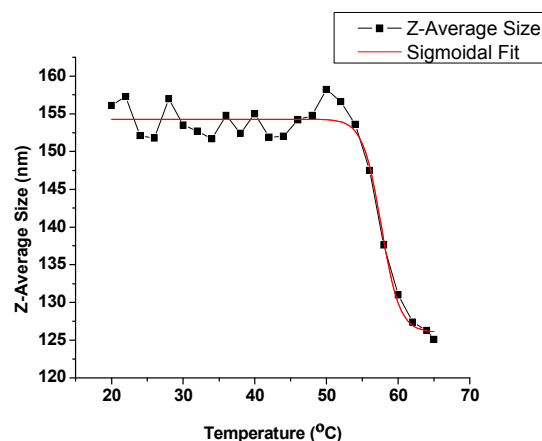


Fig.1 Plot of particle size of the SLNs against temperature.

Studies on the morphology of SLNs

The particle size and shape of SLNs was observed by TEM and non-contact mode AFM imaging. The representative TEM images of negatively stained SLNs without paliperidone loading and with paliperidone loading are shown in Figure 2a and 2b respectively. Sphere shaped SLNs of diameter in the range of 150 nm to 250 nm were

observed in TEM images. There were some poorly stained white spots observed in SLNs loaded with paliperidone. These may be due to the presence of paliperidone on the surface of SLNs. Paliperidone may not have any staining of it by Phosphotungstic Acid (PTA), which results in white spots in paliperidone loaded SLNs. PTA can work as

negative stain because it contains heavy metal ions. It can interact specifically with certain functional groups such as carboxylate, hydroxyl and amides [21]. PTA may be specifically interacting strongly with the polar functional groups of the surfactant, whereas there may not be any such interaction possible with paliperidone.

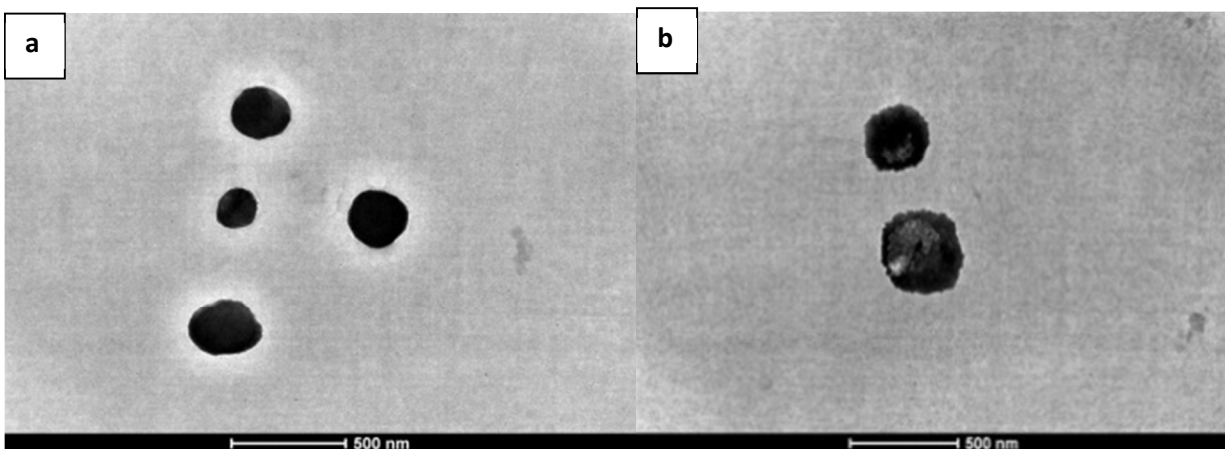


Fig. 2 HRTEM images of Gelucire® 50/13 based (a) SLNs without paliperidone and (b) SLNs loaded with paliperidone

3-dimensional structure of SLNs was studied by using non-contact mode AFM imaging. The AFM images of paliperidone loaded SLNs are shown in Figure 3. Spherical SLNs were observed with almost similar particle size. The particles were observed with their individuality intact and no agglomeration was observed in both TEM and AFM

images. This is important as we have redistributed dried SLN powder in water to prepare the suspensions for TEM and AFM imaging. Thus, TEM and AFM imaging revealed that the particles do not get agglomerated even after drying and storage. DLS, TEM and AFM data confirmed that the size of SLNs is in the range of 150 nm to 250 nm.

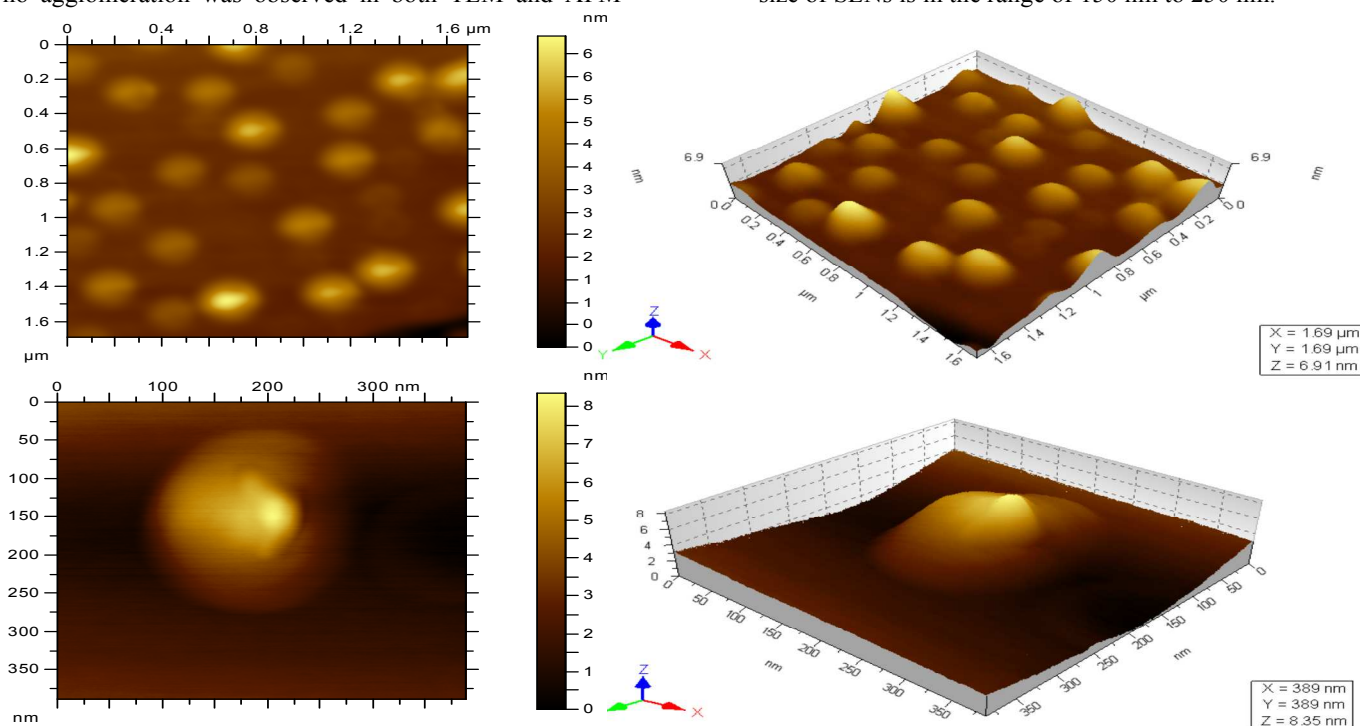


Fig. 3 AFM topography images of Gelucire® 50/13 stabilized paliperidone loaded SLNs showing homogeneous distribution of nanoparticles

In our previous study, we observed that the sodium deoxycholate stabilized SLNs were doughnut in shape [9]. The Gelucire® 50/13 stabilized SLNs in the present study

are spherical. This change in shape with change in surfactant may be due to the nature of the surfactant. Sodium deoxycholate is anionic in nature whereas

Gelucire® 50/13 is non-ionic in nature. The surfactant may be affecting the crystallinity of the lipid and thus directing the shape of the SLNs. Some studies on the effect of crystallization on shape of SLNs showed that the surfactant can influence the crystallinity and shape[22].

Physico-Chemical Characterization of SLNs

Compatibility and interaction of the ingredients determine the physico-chemical properties of the SLNs. Powder XRD of pure ingredients as well as SLNs (loaded with paliperidone and without paliperidone) are shown in Figure 4. Gelucire® 50/13 and Capmul® GMS-50K have triclinic subshell packing and the XRD patterns matched well with the already reported data [23]. Both Gelucire® 50/13 and Capmul® GMS-50K have lipid like XRD pattern with polymeric chain of macrogol. XRD pattern of paliperidone has the most intense peak at 14.6° with other characteristic peaks as reported in literature. [24]. XRD pattern of SLNs without paliperidone showed triclinic subshell packing in β polymorphic form with two prominent peaks at 19° and 23° . SLNs loaded with paliperidone also showed similar XRD pattern and hence similar crystal structure to that of SLNs without paliperidone.

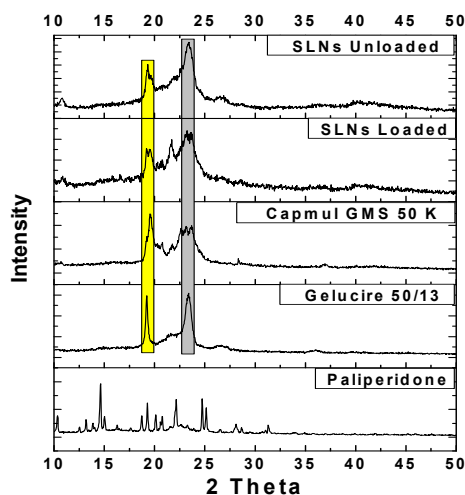


Fig. 4 XRD patterns of paliperidone, Gelucire® 50/13, Capmul® GMS-50K, SLN loaded with paliperidone and SLN without paliperidone

Relative crystallinity of the samples was calculated by area under curve method and the data is reported in Table 2. The results showed that SLNs loaded with paliperidone have lower crystallinity with respect to initial lipid matrix. Prominence of the peak at 23° increased relative to the peak at 19° in SLNs when compared to the XRD pattern of the lipid. Characteristic peaks for paliperidone was completely absent in SLNs. This shows that the drug is either molecularly dispersed in the lipid matrix or is present in the amorphous form. This is highly desirable as this might enhance solubility and bioavailability of the drug.

Table 2 Absolute and relative crystallinity of SLNs relative to Capmul® GMS-50K.

Sr. No.	Sample	Absolute crystallinity (%)	Relative Crystallinity (%)
1.	Capmul® GMS 50K	64.6	100
2.	SLNs without Paliperidone	64.0	98.9
3.	SLNs with Paliperidone	30.6	47.3

1.	Capmul® GMS 50K	64.6	100
2.	SLNs without Paliperidone	64.0	98.9
3.	SLNs with Paliperidone	30.6	47.3

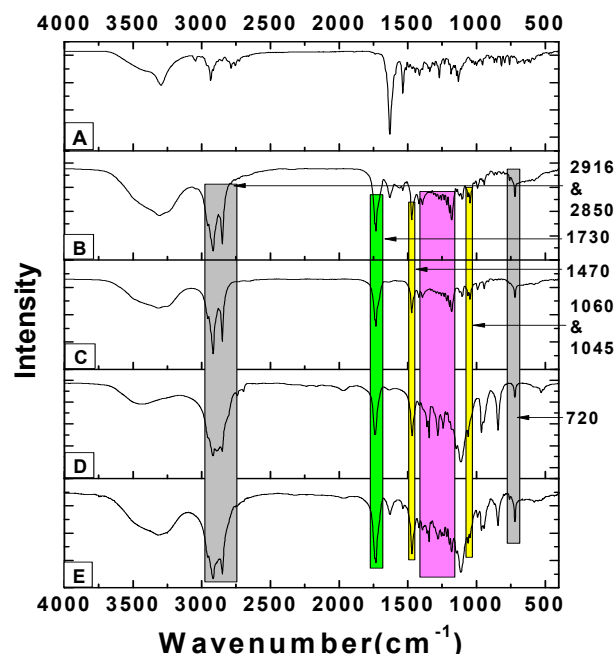


Fig. 5 FTIR spectra of (A) Paliperidone, (B) Capmul® GMS-50K, (C) Gelucire® 50/13, (D) SLNs without paliperidone and (E) SLNs loaded with paliperidone.

FTIR spectra of SLNs and the pure ingredients are shown in Figure 5. Single band at 720 cm^{-1} corresponding to CH_2 rocking vibration in triclinic subshell packing was found in the spectra for SLNs, pure lipid and the surfactant [25]. Splitting of this band occurs when the crystal structure is orthorhombic [25]. The presence of triclinic subshell packing was thus confirmed further as there was no splitting of this band in SLNs. CH_2 wagging vibration in the region due to adjacent polar end groups from 1380 cm^{-1} to 1180 cm^{-1} may help in determination of chain length of polymethylene. Stearate ester in the lipid, surfactant and the SLNs was confirmed by the single band at 1174 cm^{-1} due to C-O stretching. C=O stretching in the triglyceride ester was observed at 1730 cm^{-1} in the SLNs, in pure lipid and the surfactant. No unique and distinct peak was present in the SLNs and there was no shifting of the peaks compared to the pure lipid and the surfactant. This clearly shows that there was no chemical interaction between the drug and the excipients.

DSC thermal curves for the drug and pure excipients are shown in Figure 6 along with the thermal curves for SLNs loaded with paliperidone and the DSC curve for a physical mixture of the lipid and surfactant. All the samples showed one or more endothermic phase transitions. An endotherm starting from 56°C with a peak at 66°C and another hump at 72°C was observed for pure Capmul® GMS-50K.

Gelucire® 50/13 has an endothermic phase transition starting at 40 °C with the peak temperature at 48 °C. This corresponds to melting. An endotherm was observed for paliperidone at 172 °C. The melting point of paliperidone is reported to be in the range of 166-172°C [26]. The thermal response of the SLNs was more or less similar to the physical mixture. SLNs showed three melting peaks at 46 °C, 53 °C and 61 °C. These correspond to crystalline melting of Gelucire® 50/13 and the two-stepped melting of Capmul® GMS-50K respectively. The outer polymeric shell which has low melting point will melt first followed by Capmul® GMS-50K as shown in Figure 6. Melting point of the SLNs was relatively lower than the melting temperature of the bulk material. This may be because of the small particles size of SLNs [27]. SLNs loaded with paliperidone showed relative crystallinity as 46.2 % w.r.t. Capmul GMS 50K computed by area under curve method, which was found to be very close to the value calculated by XRD. SLNs loaded with paliperidone did not show any peak due to paliperidone melting because paliperidone becomes solubilized in the molten lipid matrix.

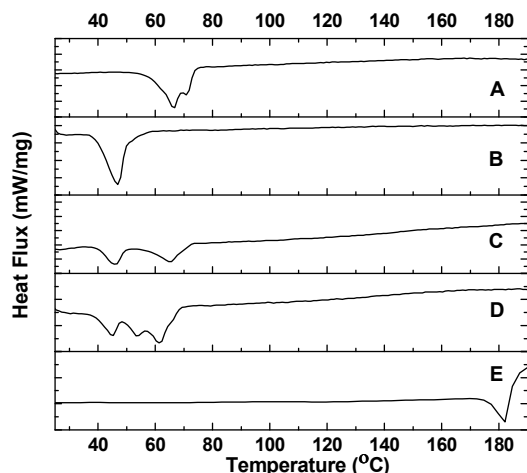


Fig. 6 DSC thermal curves of (A) Capmul® GMS-50K, (B) Gelucire® 50/13, (C) physical mixture, (D) SLNs loaded with paliperidone and (E) Paliperidone.

Entrapment Efficiency and Percentage Drug Loading

Determination of entrapment efficiency was performed by UV-visible spectroscopy. Paliperidone has very good solubility in acidic medium [9]. Hence, 0.1N HCl solution was used to dissolve paliperidone selectively from the SLNs. Centrifugation was used to separate nanoparticles from the acidified dispersion. The concentration of free drug after dissolution was found to be 0.248 mg/ml. The entrapment efficiency and the drug loading were calculated to be 75% and 7% respectively. Gelucire® 50/13 stabilized SLNs seems to be better in terms of increasing the drug loading and entrapment efficiency than sodium deoxycholate stabilized SLNs [17]. This is primarily because; higher concentration of Gelucire® 50/13 can be used to form the SLNs, whereas sodium deoxycholate is limited by its toxicity at high concentration. Lower relative crystallinity of Gelucire® 50/13 stabilized SLNs with

respect to the bulk lipid can also be a reason for high entrapment efficiency and high drug loading [28].

Experimental

Materials

Capmul® GMS-50K was provided by Abitech USA as a gift sample. Gelucire® 50/13 pellets were provided by Gattefosse France also as a gift sample. Double distilled water from Bioage water purification system was used in all the preparations and washing. Hydrochloric acid, potassium bromide, sodium chloride, Sodium dihydrogen phosphate and Disodium hydrogen phosphate were purchased from Fischer chemicals.

Methods

Preparation of Gelucire® 50/13 stabilized SLNs with and without paliperidone

Melt homogenization and self-emulsification was utilized to obtain the Gelucire® 50/13 stabilized SLNs [29]. Preparation of SLNs involved three steps. Appropriate quantity of Capmul® GMS-50K and Gelucire® 50/13 was primarily weighed and heated to 75 °C so that the whole mixture melts completely. Paliperidone was subsequently weighed and suspended in molten lipid through stirring at 75 °C. Afterwards water was added to drug-lipid-stabilizer mixture by incessant stirring to make a pre-emulsion. The pre-emulsion was further homogenized by ultrasound homogenizer to trim down the particle size to nanosize range. The hot micro-emulsion was cooled slowly up to 4 °C for solidification. A series of formulations with varying concentration of stabilizer were prepared. Extra amounts of stabilizer was removed by centrifugation at 10000 RPM for 2 hours and particle pellets obtained was dried in vacuum oven at 40 °C to obtain dried samples for further analysis.

Z-average size/Hydrodynamic diameter measurement

Photon correlation spectroscopy/dynamic light scattering measurement was done by using Zetasizer Nano ZS (Malvern Instruments, Malvern, UK) having 632.8 nm red laser with a detector angle of 173°. DLS measurements of diluted samples were done in glass cell with round aperture at 25 °C with 120 s incubation time. Cumulant analysis method was used to compute the autocorrelation function. Data recorded in triplicate and mean was plotted. Mean value of size (Z-average) and a width parameter known as polydispersity index (Pdi) are reported.

Effect of Gelucire 50/13 content on size of SLNs

SLNs were prepared at varying quantities of Gelucire® 50/13 from 2.5 mg/ml to 20 mg/ml with 2.5 mg/ml increment to each sample in 40 ml of water. Ratio (wt/wt.) of Gelucire® 50/13 to Capmul® GMS-50K was 1:4, 1:2, 3:4, 1:1, 5:4, 3:2, 7:4 and 2:1. Samples were prepared by the method as described above. Amount of all other components like Capmul® GMS-50K, paliperidone and water remained a constant in all the samples. All the preparation parameters were maintained the same to remove the effect of process parameters on the size of SLNs.

Transmission electron microscopy

Tecnai G20 S-Twin of FEI, USA was used to obtain high resolution transmission electron microscopy images at 200 kV. Sample drop was incubated for 90 s and dried on carbon coated copper grids. They were further stained by 2.5% phospho-tungstic acid (PTA) for another 90 s. Excess stain was removed by washing of samples with purified water. Images were obtained in dark field as well as bright field mode at different magnifications.

Atomic force microscopy

Low frequency silicon cantilever (Force Constant: 21 N/m to 98 N/m) at frequency 146 kHz to 236 kHz was used with a closed loop scanner in SPM 5500 (Agilent) system to acquire the non-contact mode AFM images. Pico image software was used for the filtration and 3D study of AFM data.

X-ray diffraction

Panalytical Xpert Pro was used to record the XRD pattern of processed powder samples. The data was collected in the 2θ range of 10-50° with a scan step size of 2°. Cu K_{α1} with λ=1.54060 Å was used as anodic material.

FTIR spectroscopy

Dried powder samples were pelletized along with KBr powder for FTIR measurement. FT-IR spectra were logged by Perkin-Elmer Spectrum 65 spectrophotometer in the range 4000-400 cm⁻¹ at a resolution of 1 cm⁻¹.

Differential scanning calorimetry (DSC) analysis

Small quantities of samples were analyzed by Netzsch STA 449 F1 in hermetically sealed aluminium pans for DSC measurements at the heating rate of 2 °C/min from 25 °C to 200 °C under N₂ flow at the rate of 60 ml/min.

% Entrapment Efficiency (%EE) and % Drug Loading (%DL) Determination

Free paliperidone present in SLN dispersion was solubilized by 0.1N HCl and centrifugation was used to separate out SLNs from the supernatant. Supernatant was further filtered through 0.45µm syringe filter to obtain a clear solution. Concentration of paliperidone was quantified using UV-Visible-NIR spectrophotometer. λ_{max} at 238 nm was used to plot the standard curve (10-50 µg/ml) for the determination of paliperidone concentration in the filtrate. The formula mentioned below was used to compute %EE and %DL [30]. The weight in mg was used in the formula and PPN refers to paliperidone.

$$\%EE = \frac{(\text{Total PPN}) - (\text{Free PPN})}{(\text{Total PPN})} \times 100$$

$$\%DL = \frac{(\text{Total PPN}) - (\text{Free PPN})}{(\text{Total PPN}) + (\text{Total Lipid}) - (\text{Free PPN})} \times 100$$

Conclusions

Gelucire® 50/13 when used as a surfactant to prepare the SLNs influences the particle size. Particle size of SLNs decreases with increase in concentration of Gelucire® 50/13. The Gelucire® 50/13 stabilized SLNs have good entrapment efficiency and drug loading. Particle size of

SLNs was found to be small enough (150 nm to 250 nm) for the use as nanodrug delivery system. Optimised SLN formulation with smaller particle size as compared to Sodium deoxycholate stabilized SLNs can be obtained by using Gelucire(R) 50/13 as surfactant. Entrapment efficiency and % drug loading of these SLNs was found to be 75% and 7% respectively which is better than sodium deoxycholate stabilized SLNs. The SLNs have relatively lower crystallinity as compared to the bulk lipid. Molecular solid solution of paliperidone was confirmed by XRD, DSC and FTIR analysis.

Acknowledgements

Authors acknowledge NIT Hamirpur for providing the laboratory facilities and MHRD (Govt. of India) for financial support. Authors also acknowledge IIT Mandi for providing DSC and TEM facilities.

Notes and references

Centre for Material Science and Engineering, National Institute of Technology Hamirpur, Himachal Pradesh-177005, India

‡ Presently at: School of Engineering, Indian Institute of Technology Mandi, Himachal Pradesh-175005, India.

Email: jaspreet@iitmandi.ac.in.

Phone Number: +919418085224

- [1] B.L. Roth, D.J. Sheffler, W.K. Kroeze, *Nat Rev Drug Discov*, 3 (2004) 353-359.
- [2] K. Packard, P. Price, A. Hanson, *Journal of Pharmacy Practice*, (2014).
- [3] R. Hunter, *Advances in Psychiatric Treatment*, 20 (2014) 3-12.
- [4] A.M. Palmer, *Journal of Alzheimer's Disease*, 24 (2011) 643-656.
- [5] A. Boer, P. Gaillard, *Clin Pharmacokinet*, 46 (2007) 553-576.
- [6] S. Kumar, J.K. Randhawa, *Materials Science and Engineering: C*, 33 (2013) 1842-1852.
- [7] J. de Leon, G. Wynn, N.B. Sandson, *Psychosomatics*, 51 (2010) 80-88.
- [8] E. Dremencov, M. El Mansari, P. Blier, *Psychopharmacology*, 194 (2007) 63-72.
- [9] H.-J. Zhu, J.-S. Wang, J.S. Markowitz, J.L. Donovan, B.B. Gibson, C.L. DeVane, *Neuropsychopharmacology*, 32 (2006) 757-764.
- [10] J. Greenwood, J. Adu, A.J. Davey, N.J. Abbott, M.W.B. Bradbury, *J Cereb Blood Flow Metab*, 11 (1991) 644-654.
- [11] D.-J. Jang, S.T. Kim, K. Lee, E. Oh, *Bio-Medical Materials and Engineering*, 24 (2014) 413-429.
- [12] S. Shimpi, B. Chauhan, K.R. Mahadik, A. Paradkar, *Pharmaceutical Research*, 22 (2005) 1727-1734.
- [13] N. Passerini, B. Perissutti, M. Moneghini, D. Voinovich, B. Albertini, C. Cavallari, L. Rodriguez, *Journal of Pharmaceutical Sciences*, 91 (2002) 699-707.
- [14] M. El-Badry, G. Fetih, M. Fathy, *Saudi Pharmaceutical Journal*, 17 (2009) 217-225.
- [15] V.V. Ranade, J.B. Cannon, *Drug Delivery Systems*, Third Edition, Taylor & Francis, 2011.

- [16] S. Kumar, J. Kaur, AIP Conference Proceedings, 1536 (2013) 163-164.
- [17] S. Kumar, J.K. Randhawa, Colloids and Surfaces B: Biointerfaces, 102 (2013) 562-568.
- [18] S. Tcholakova, N.D. Denkov, T. Danner, Langmuir, 20 (2004) 7444-7458.
- [19] M.J. Schick, Nonionic Surfactants: Physical Chemistry, Taylor & Francis, 1987.
- [20] T. Helgason, T.S. Awad, K. Kristbergsson, E.A. Decker, D.J. McClements, J. Weiss, Journal of Agricultural and Food Chemistry, 57 (2009) 8033-8040.
- [21] L. Sawyer, D. Grubb, G.F. Meyers, Polymer Microscopy, Springer, 2008.
- [22] K. Jores, W. Mehnert, M. Drechsler, H. Bunjes, C. Johann, K. Mäder, Journal of Controlled Release, 95 (2004) 217-227.
- [23] K. Sato, Chemical Engineering Science, 56 (2001) 2255-2265.
- [24] S. Ini, K. Chen, E. Lancry, N. Chasid, Y. Shmueli, B.Z. Dolitzky, in, Google Patents, 2009.
- [25] D. Chapman, Journal of the American Oil Chemists' Society, 42 (1965) 353-371.
- [26] F. Sun, Z. Su, C. Sui, C. Zhang, L. Yuan, Q. Meng, L. Teng, Y. Li, Basic & Clinical Pharmacology & Toxicology, 107 (2010) 656-662.
- [27] H. Bunjes, M.H.J. Koch, K. Westesen, Journal of Pharmaceutical Sciences, 92 (2003) 1509-1520.
- [28] D. Hou, C. Xie, K. Huang, C. Zhu, Biomaterials, 24 (2003) 1781-1785.
- [29] A. Kale, V. Patravale, AAPS PharmSciTech, 9 (2008) 191-196.
- [30] A.E. Yassin, M.K. Anwer, H.A. Mowafy, I.M. El-Bagory, M.A. Bayomi, I.A. Alsarra, International journal of medical sciences, 7 (2010) 398-408.